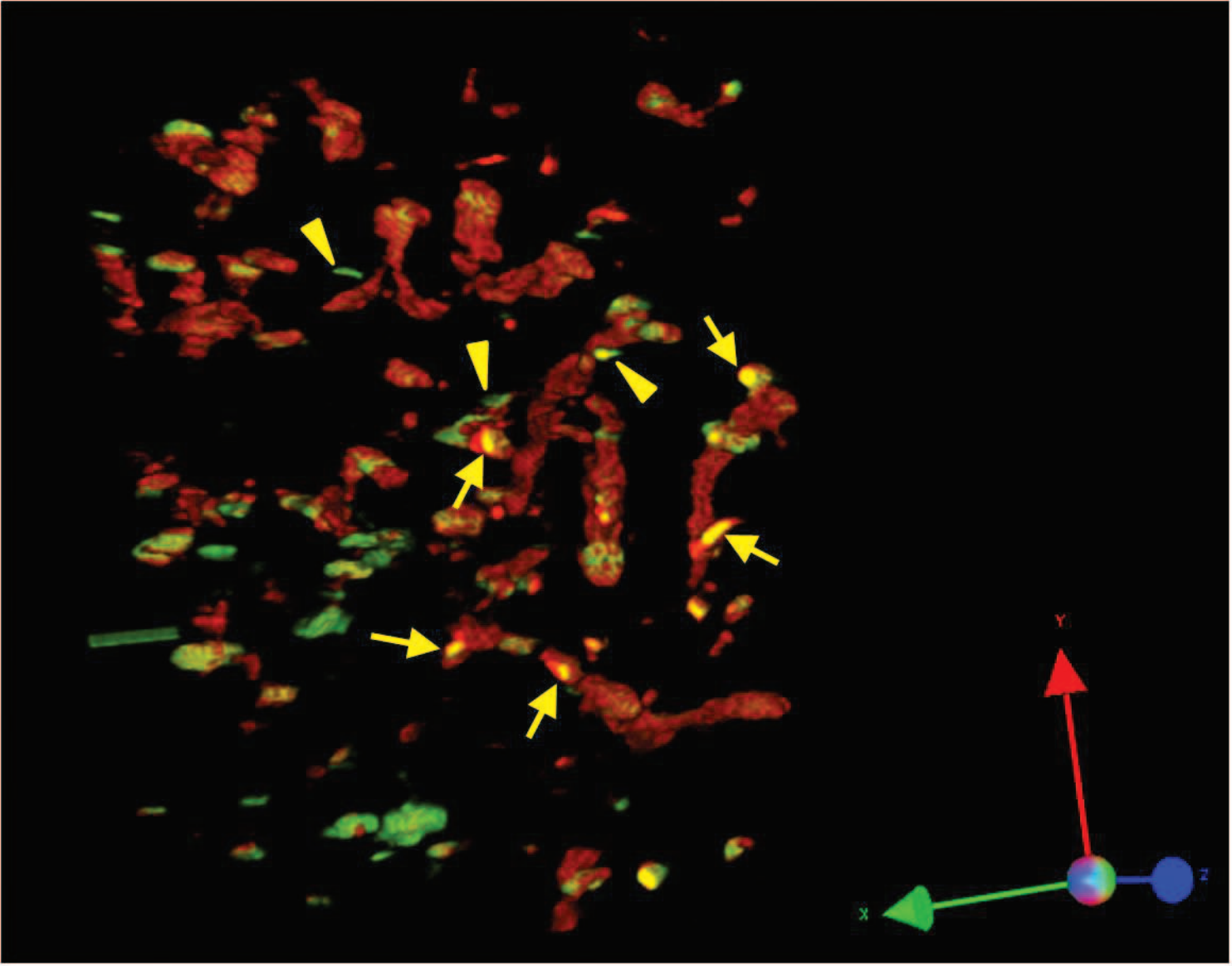

Nature Immunology: doi:10.1038/ni.1855

Suppl Fig. 1

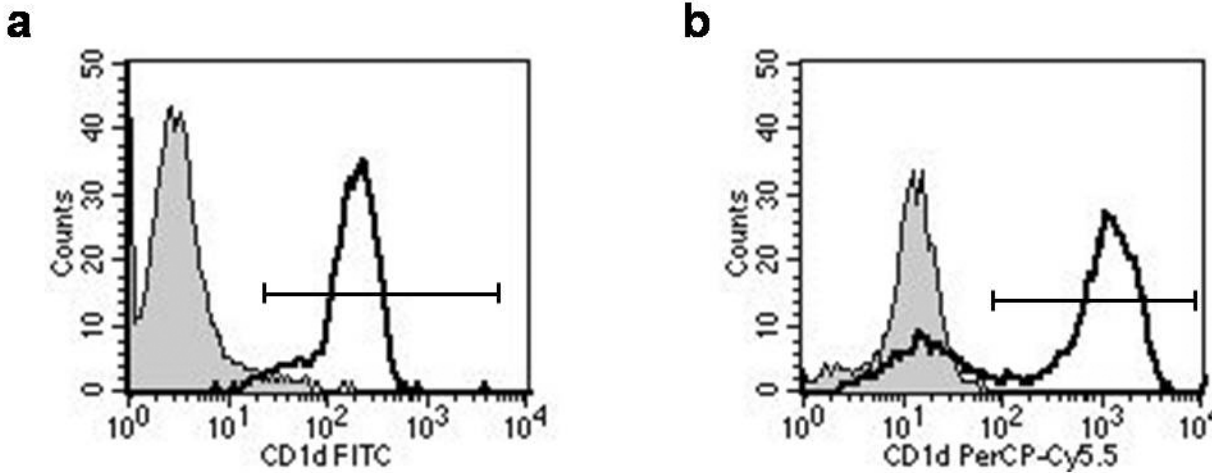

Nature Immunology: doi:10.1038/ni.1855

Suppl Fig. 2

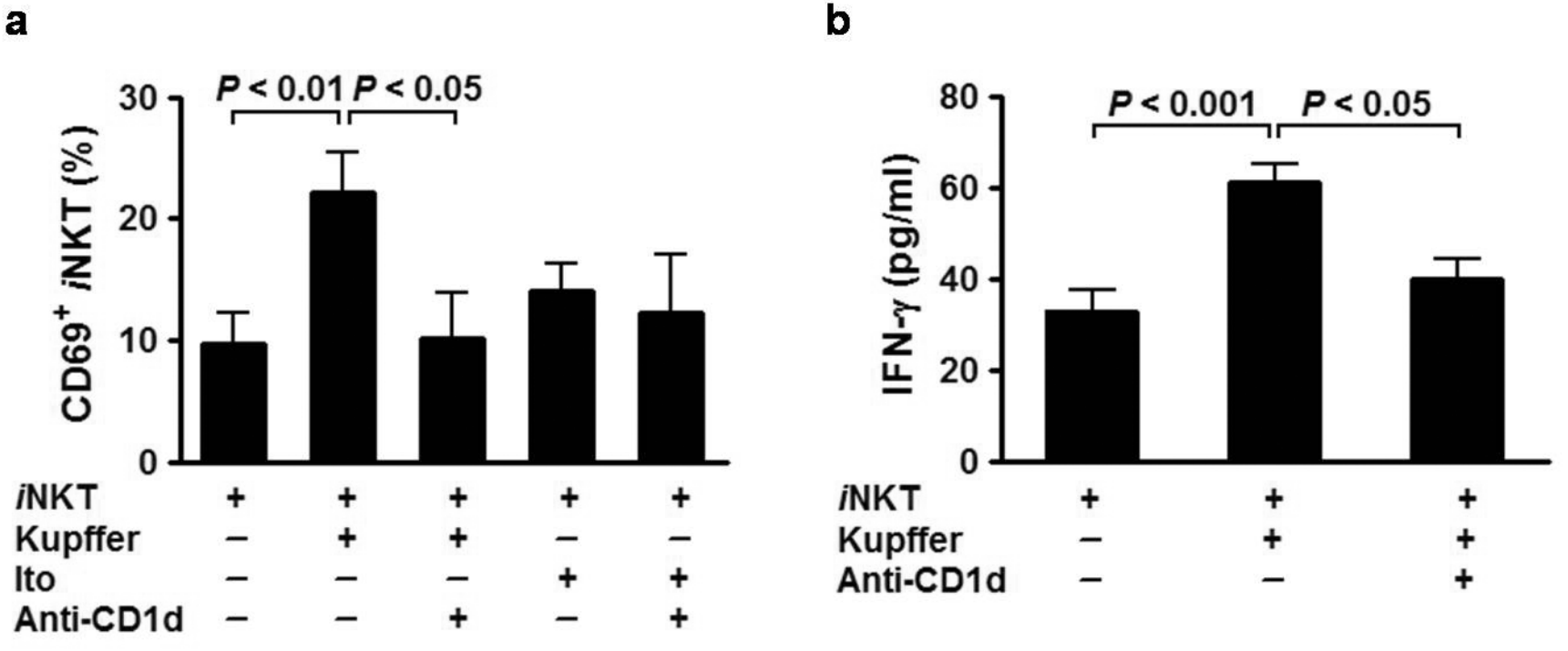

Nature Immunology: doi:10.1038/ni.1855

Suppl Fig. 3

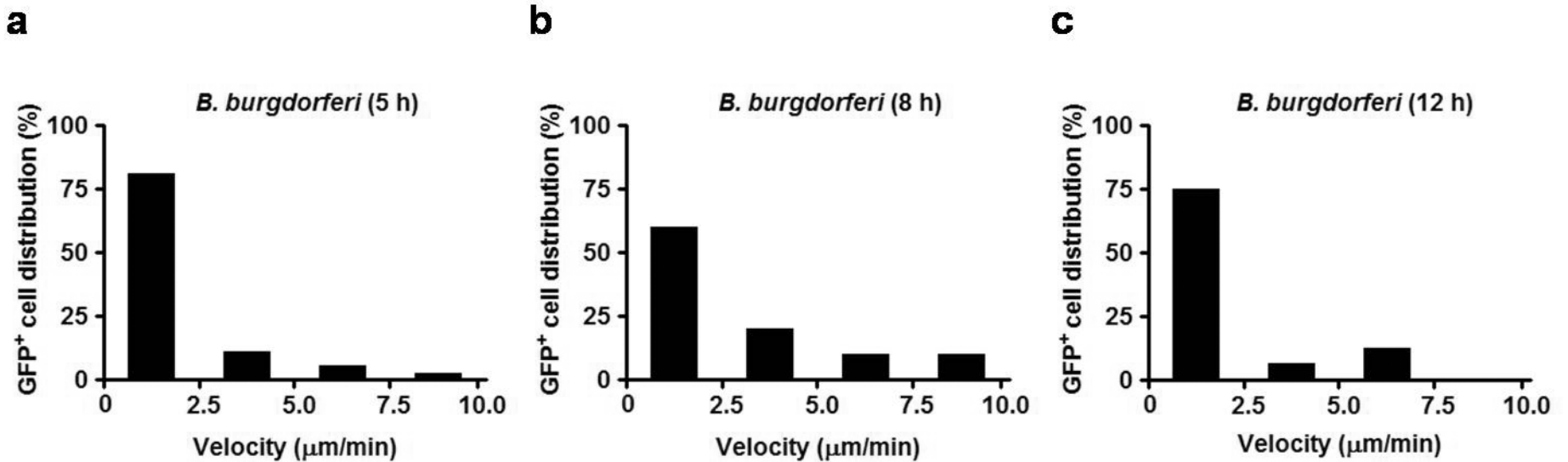

Nature Immunology: doi:10.1038/ni.1855

Suppl Fig. 4

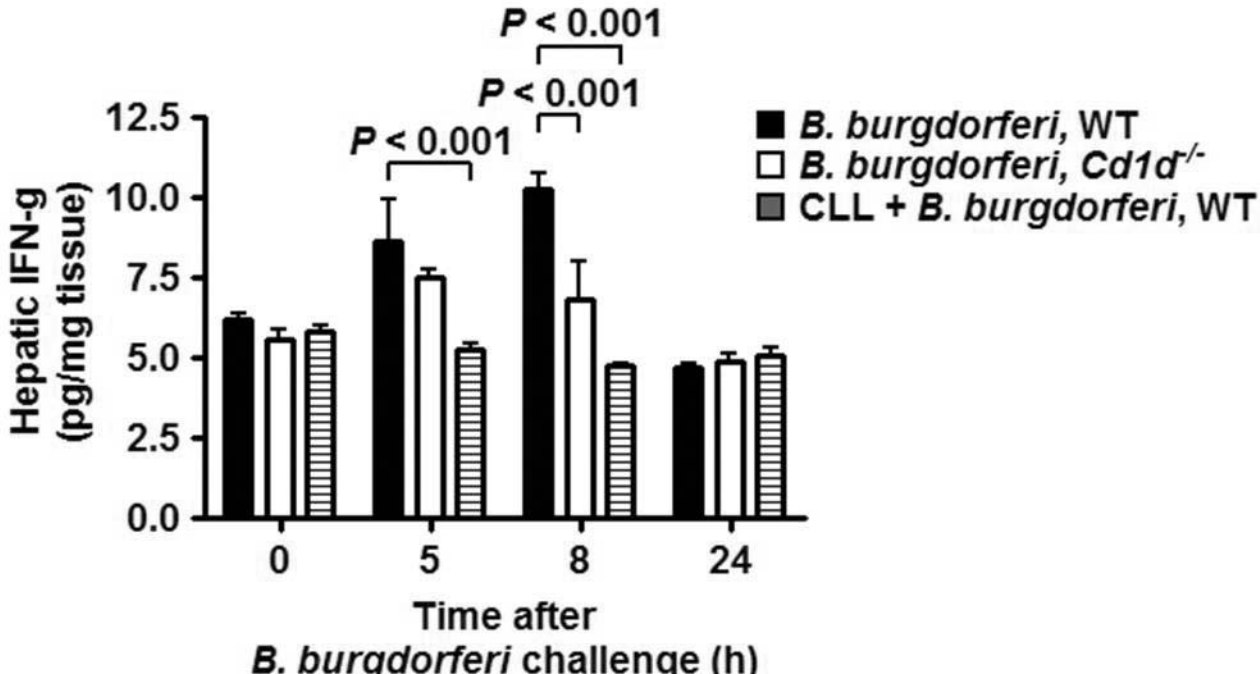

Nature Immunology: doi:10.1038/ni.1855

Suppl Fig. 5

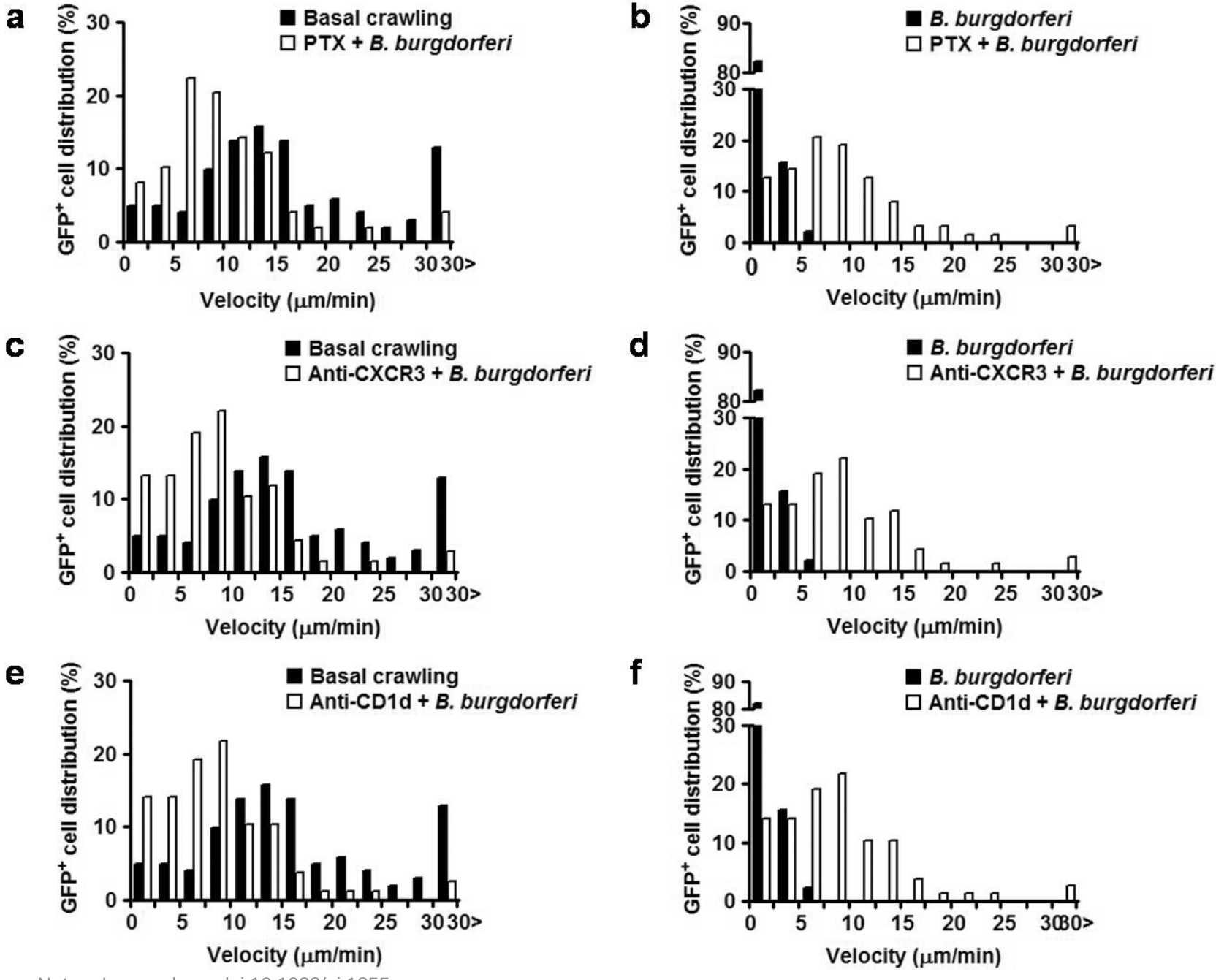

Nature Immunology: doi:10.1038/ni.1855

Suppl Fig. 6

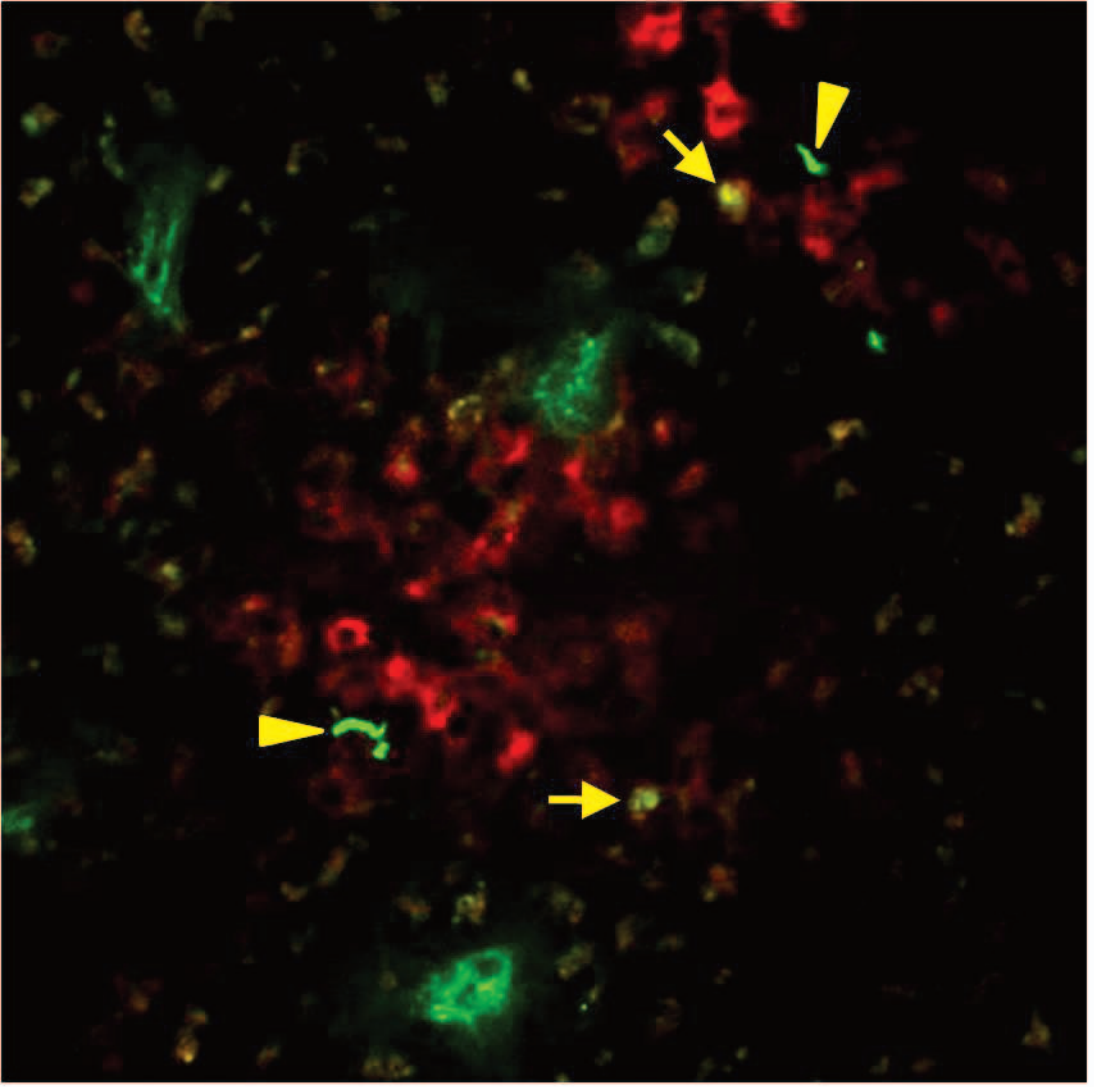

Nature Immunology: doi:10.1038/ni.1855

Suppl Fig. 7

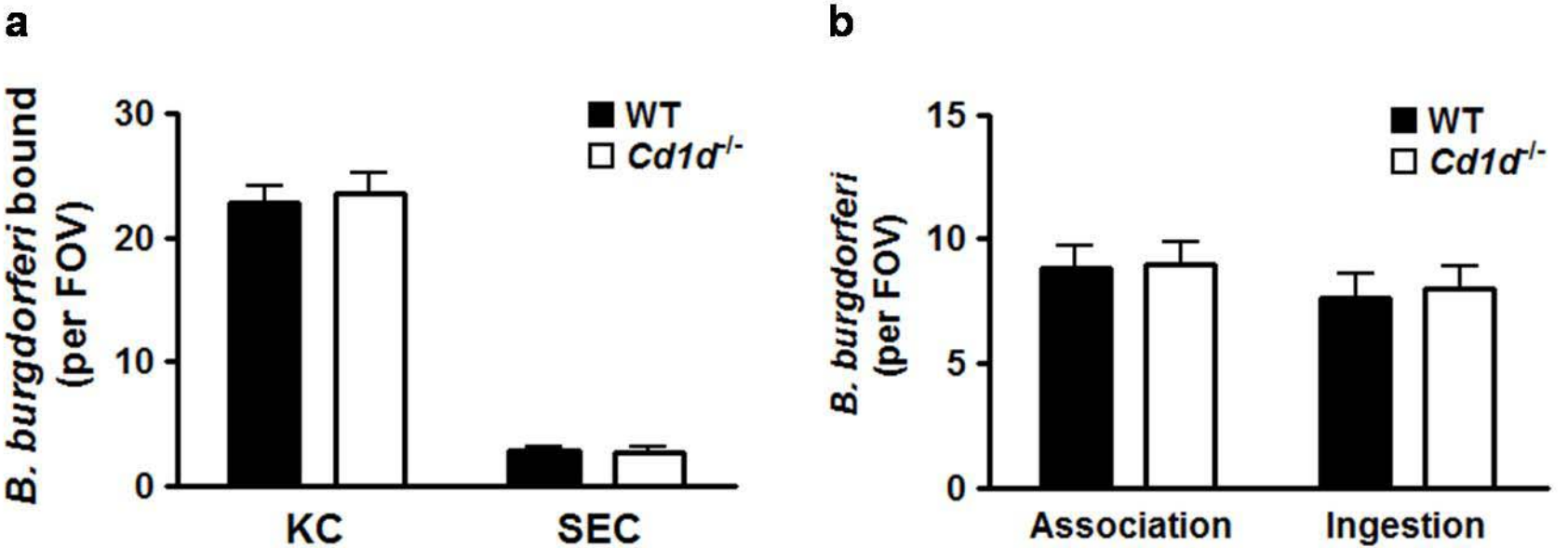

Nature Immunology: doi:10.1038/ni.1855

Suppl Fig. 8

Supplementary Table 1. Liver as the primary site of *B. burgdorferi* localization in mice

	B. burgdorferi flaB (10^3 copies in the whole organ or tissue)				
	Blood	Bladder	Heart	Liver	Spleen
WT	27.8 ± 4.1	274.4 ± 3.9	1,910.1 ± 15.6	21,446.4 ± 8747.1	1,395.8 ± 101.5
CLL, WT	109.7 ± 2.9***	830.4 ± 4.0***	2,960.7 ± 138.6**	46,166.4 ± 5076.7	5,631.2 ± 772.9*
Splenectomized, WT	9.1 ± 4.6	219.0 ± 19.6	1,664.7 ± 111.3	29,669.0 ± 980.8	-
Cd1d$^{-/-}$	5.6 ± 4.6	450.2 ± 28.2*	998.6 ± 18.4*	39,873.7 ± 1258.1	1,908.3 ± 109.2

Bacterial load in untreated, CLL-treated or splenectomised wild-type mice and in *Cd1d*$^{-/-}$ mice at 3 d after *B. burgdorferi* infection, assessed by quantitative PCR analysis of *B. burgdorferi flaB* (pooled DNA samples). *$P < 0.05$, **$P < 0.01$, ***$P < 0.001$, versus wild-type (Bonferroni's multiple comparison test). Data represent one experiment with three to five mice, depending on experimental group (mean and s.e.m. of two independent measurements).

SUPPLEMENTARY FIGURE LEGENDS

Supplementary Figure 1. The *z*-stack reconstruction of *Cxcr6*$^{gfp/+}$ liver at 2 h after GFP-expressing *B. burgdorferi* injection. Kupffer cells were labeled with phycoerythrin-conjugated anti-F4/80. This tool allowed determination of attachment (arrowheads) versus ingestion (arrows) of spirochetes. Original magnification, ×10. Data represent three independent experiments.

Supplementary Figure 2. CD1d expression by Kupffer cells and Ito cells. Kupffer cells (**a**) and Ito cells (**b**) isolated from BALB/c mice infected by *B. burgdorferi* were labeled with FITC- and PerCP-Cy5.5-conjugated anti-CD1d, respectively. Data are representative of two independent experiments.

Supplementary Figure 3. *i*NKT activation induced by Kupffer cells or Ito cells, infected by *B. burgdorferi*. Kupffer cells or Ito cells were cocultured with naïve *i*NKT cells isolated from *Cxcr6*$^{gfp/+}$ livers and spleens in DMEM containing 10% FCS. IFN-γ concentrations (**b**) in supernatant at 4 d after coculture, and the CD69 expression of *i*NKTs at 24 h (**a**), and 4 d (see **Fig. 4c**) were quantified. *P* values, unpaired Student's *t*-test (**a**) and Bonferroni's multiple comparison test (**b**). Data are representative of three independent experiments (**a,b**; error bars, s.e.m.).

Supplementary Figure 4. Effect of *B. burgdorferi* on the crawling velocity of *i*NKT cells. At 5 h (**a**), 8 h (**b**), and 12 h (**c**) after *B. burgdorferi* injection into *Cxcr6*$^{gfp/+}$ mice,

CXCR6^{+} cell tracks were analyzed from ×10 magnification videos (see **Fig. 5b** for 24 h post-infection results). Data are representative of more than two independent experiments.

Supplementary Figure 5. Hepatic concentrations of IFN-γ. Enzyme-linked immunosorbent assay of IFN- γ in liver tissue homogenate obtained from untreated, CLL-treated wild-type (WT) or *Cd1d*$^{-/-}$ mice before or 5, 8, or 24 h after *B. burgdorferi* infection. *P* values, Bonferroni's multiple comparison test. Data are representative of one experiment with four to six mice per group (error bars, s.e.m.).

Supplementary Figure 6. Profound change in *i*NKT cell activity by *B. burgdorferi* infection. (**a-f**) Effect of PTX, anti-CXCR3, and anti-CD1d on *i*NKT cells activity in *B. burgdorferi* infection. The crawling velocity distribution of CXCR6^{+} *i*NKT cells in *Cxcr6*$^{gfp/+}$ mice was compared to basal crawling (**a,c,e**), and to *B. burgdorferi* alone group (**b,d,f**) at 24 h after infection. Data are representative of more than ten FOV of three independent experiments (basal crawling) or more than six FOV two independent experiments (blocker-treated**)**.

Supplementary Figure 7. *B. Burgdorferi* clearance by spleen. At 2 h after GFP-expressing *B. burgdorferi* infection, some spirochetes were stationary in spleen (arrows) and a few were co-localized with splenic macrophages (arrowheads). Original magnification, ×20. Data are representative of ten FOV from two independent experiments.

Supplementary Figure 8. Phagocytic capacity in the liver of wild-type and *i*NKT deficient mice. The number of bound GFP-expressing *B. burgdorferi* to Kupffer cells and endothelium was counted at 1-2 hr after intravenous injection (a; see Fig. 2,3 legends and Supplementary Methods). Interaction and ingestion of the GFP spirochetes by red-labeled Kupffer cells were measured from intravital videos and *Z*-stack reconstruction pictures of the BALB/cj and *Cd1d*$^{-/-}$ mice. Dara are representative of more than 10 FOVs from two independent experiements.

SUPPLEMENTARY VIDEO LEGENDS

Supplementary Video 1. Distribution and movement of *i*NKT cells in the hepatic sinusoids of *Cxcr6*$^{gfp/+}$ mouse. Low magnification (×4) video shows the general crawling pattern of *i*NKT cells. Experimental conditions were as described in the **Figure 1a** legend and in more detailed **Supplementary Methods**. Elapsed time is shown at the top right. The time lapse was recorded at 0.3 fps and exported to video at 30 fps.

Supplementary Video 2. *i*NKT cell movement in the hepatic sinusoids of *Cxcr6*$^{gfp/+}$ mouse. Intermediate magnification (×10) video shows the general crawling pattern of *i*NKT cells. Experimental conditions were as described in the **Figure 1b** legend and in more detailed **Supplementary Methods**. Elapsed time is shown at the top right. The time lapse was recorded at 0.3 fps and exported to video at 30 fps.

Supplementary Video 3. Differential behavior of *i*NKT cells and Kupffer cells in the hepatic sinusoids of *Cxcr6*$^{gfp/+}$ mouse. Intermediate magnification (×10) video shows the

procedure of Kupffer cell labelling and behavioral patterns of *i*NKT cells/Kupffer cells. Experimental conditions were as described in the **Supplementary Methods**. Elapsed time is shown at the top right. The time lapse was recorded at 0.3 fps and exported to video at 30 fps.

Supplementary Video 4. Distribution and behavior of *i*NKT cells. Intermediate magnification (×10) video shows that *i*NKT cells are localized widely within sinusoids, but rarely in venules. *i*NKT cells that attempted to move into post-sinusoidal venule were often swept away (indicated by arrow). Experimental conditions were as described in the **Supplementary Methods**. Elapsed time is shown at the top right. The time lapse was recorded at 0.3 fps and exported to video at 30 fps.

Supplementary Video 5. Filtering function of Kupffer cells in the hepatic sinusoids I. High magnification (×20) video shows the typical binding pattern of foreign molecules between Kupffer cells and beads. Experimental conditions were as described in the **Figure 1c**, **2a** and **2b** legends and in more detailed **Supplementary Methods**. Elapsed time is shown at the top right. The time lapse was recorded at 0.3 fps and exported to video at 30 fps.

Supplementary Video 6. Strikingly different behaviour for *B. burgdorferi* attached to Kupffer cells and endothelium. High magnification (×20) video shows that *B. burgdorferi* bound to Kupffer cells were relatively immobilized (indicated by arrow) when compared to endothelium (indicated by arrowhead; moved back and forth over 10-20 μm).

Experimental conditions were as described in the **Supplementary Methods**. Elapsed time is shown at the top right. The time lapse was recorded at 0.3 fps and exported to video at 30 fps.

Supplementary Video 7. The cluster formed by *i*NKT cells 24 h after *B. burgdorferi* treatment I. Intermediate magnification (×10) video shows a big *i*NKT cluster at 24 h after *B. burgdorferi* treatment. Experimental conditions were as described in the **Figure 5f** legend and in more detailed **Supplementary Methods**. Elapsed time is shown at the top right. The time lapse was recorded at 0.3 fps and exported to video at 30 fps.

Supplementary Video 8. The cluster formed by *i*NKT cells 24 h after *B. burgdorferi* treatment II. High magnification (×20) video shows a big *i*NKT cluster formed on Kupffer cells 24 h after *B. burgdorferi* treatment and few spirochetes in the liver. Experimental conditions were as described in the **Figure 5f** and **5g** legend and in more detailed **Supplementary Methods**. Elapsed time is shown at the top right. The time lapse was recorded at 0.3 fps and exported to video at 30 fps.

Supplementary Video 9. Filtering function of Kupffer cells in the hepatic sinusoids II. At 12 h after *B. burgdorferi* treatment, high magnification (×20) video shows that Kupffer cell-depleted liver could not clear the pathogens. Experimental conditions were as described in the **Supplementary Methods**. Elapsed time is shown at the top right. The time lapse was recorded at 0.3 fps and exported to video at 30 fps.

Supplementary Video 10. *i*NKT crawling in anti-CD1d-treated mouse liver at 24 h after *B. burgdorferi* treatment. Intermediate magnification (×10) video shows that anti-CD1d (1B1; eBioscience) did not reduce the velocity with which the *i*NKT cells crawl in the sinusoids, while it inhibited *i*NKT cluster formation. A small cluster of *i*NKT cells is seen in the video, but *i*NKT cells are still crawling on Kupffer cells. Experimental conditions were as described in the **Methods**. Elapsed time is shown at the top right. The time lapse was recorded at 0.2 fps and exported to video at 30 fps.

SUPPLEMENTARY METHODS

Briefly, mice were anesthetized by intraperitoneal injection of a mixture of 10 mg/kg xylazine hydrochloride (MTC Pharmaceuticals) and 200 mg/kg ketamine hydrochloride (Rogar/STB). The right jugular vein was cannulated to administer additional anesthetic, beads, fluorescent dyes and/or bacteria. Body temperature was maintained at 37°C using an infrared heat lamp. Mice were placed in a right lateral position on an adjustable microscope stage. A lateral abdominal incision along the costal margin to the midaxillary line was made to exteriorize the liver, and all exposed tissues were moistened with saline-soaked gauze to prevent dehydration.

Spinning disk confocal intravital microscopy. The liver and spleen were prepared for *in vivo* microscopic observation. Briefly, the liver or spleen was placed on the pedestal of a microscope and continuously superfused with warmed bicarbonate-buffered saline (pH 7.4). The liver and spleen surface were then covered with a coverslip to hold the organ in position. The liver and spleen microvasculature were visualized using a spinning disk confocal microscope and images were acquired with an Olympus BX51 upright microscope or an Olympus IX81 inverted microscope using a ×4/0.16 UplanSApo, ×10/0.30 UplanFL N, and ×20/0.45 LUCplanFL N objectives as preveiously described[1,2]. The microscope was equipped with a confocal light path (WaveFx, Quorum) based on a modified Yokogawa CSU-10 head (Yokogawa Electric Corp.). *Cxcr6*$^{gfp/+}$ and *Cx3cr1*$^{gfp/+}$ mice were used to visualize hepatic *i*NKT cells and Ito cells/Dendritic cells in the liver, respectively. Phycoerythrin-conjugated anti- F4/80 (BM8, eBiosciences; 1 μg/mouse) was injected intravenously into wild-type and *Cxcr6*$^{gfp/+}$ mice to image Kupffer cells.

Three (488-, 561-, and 635-nm) laser excitation wavelengths (Cobalt) were used in rapid succession and visualized with the appropriate long-pass filters (Semrock). Typical exposure time for excitation wavelengths was 0.8-1.2 sec. A 512 × 512 pixel back-thinned electron-multiplying charge-coupled device camera (C9100-13, Hamamatsu) was used for fluorescence detection. Volocity acquisition software (Improvision) was used to drive the confocal microscope. Sensitivity settings were 200-240, and autocontrast was used. Images were captured at 16 bits/channel in RGB. Red, green, and blue channels were overlaid using brightest point settings before export in .tif or .avi format. Simultaneous behaviors of Kupffer cells, *i*NKT cells, and fluorescent *B. burgdorferi* in the hepatic microvasculature were assessed.

Analysis of intravital imaging videos. Cells were tracked using ImageJ software version 1.41 (NIH at http://rsb.info.nih.gov/ij/). Time-lapse video exported from Volocity was imported in .mov files, and then converted to 8-bit grayscale. Fluorescent cells were adjusted using threshold control, and noise particles less than 2.0 pixels were removed by despeckle and median filter. Movement of cells was measured using manual tracking, and was calculated for each track by manipulation of ImageJ output spreadsheets. The cell velocity was expressed in distance (μm)/time (min). Thirty to forty tracks from 5-10 min videos in each experimental group were analyzed.

Construction of Tomato expression plasmid pTM201 and GFP expression plasmid pTM61. Using overlap extension PCR, Tomato coding sequence[3] was fused to the terminator sequences (T1 × 4), *rbs* and *B. burgdorferi flaB* promoter from pCE320(*gfp*)-

P_{flaB}[4]. The terminator, *rbs*, P_{flaB} and Tomato inserts were flanked with *Sac*I and *Kpn*1 sites for cloning into the *Sac*I and *Kpn*I sites of the pBSV2g-derived *Borrelia* shuttle vector pTM49. For the first step of the Tomato cloning, the terminator/*rbs*/P_{flaB} region was amplified for 25 PCR cycles using primers B696 (5'-ccggagctcatgataagctgtcaaacatgag-3') and B1374 (5'-cctcgcccttgctcaccatatgtttttcctccttataaagtta-3'). The Tomato coding sequence was amplified for 25 PCR cycles using primers B1373 (5'-taactttataaggaggaaaaacatatggtgagcaagggcgagg-3') and B1375 (5'-ggtacctcagatctattacttgtacagctcgtccat-3'). 50 µl PCR reactions were performed using 75 ng DNA template, 5 pmoles each primer, 0.5 µl Phusion DNA polymerase (NEB), 3% DMSO, 0.1 mmol dNTPs and 10 µl 5× Phusion HF buffer (NEB). PCR conditions: 98℃ 3 min, followed by 25 cycles of 98℃ 15 sec, 63℃ 15 sec, 72℃ 30 sec, followed by 7 min at 72℃. In the second step of PCR overlap extension for the Tomato cloning, 2.5 µl of each PCR product were mixed (5 µl total), and annealing and extension was conducted for 6 cycles using the PCR conditions described above (in the absence of any PCR reaction mixture). Finally, in the third step of PCR overlap extension, 2.5 µl of the extension mixture from step two was amplified using primers B696 and B1375 (with the same PCR cycling and reaction conditions as Step 1). The final PCR product was cloned into the pJET1.2/Blunt cloning vector using the CloneJet PCR cloning kit (Fermentas), followed by *Sac*I/*Kpn*I excision of the insert and cloning into *Sac*I/*Kpn*I pTM49 to generate pTM201. Plasmid template for the Tomato sequence was pRSET-B Tomato[3]. Sequencing of the Tomato inserts revealed that the Tomato cassette contained only the last 228 amino acids of Tomato (one tomato monomer). However, this Tomato clone was

still fluorescent, and was used in all subsequent experiments. GFP expression plasmid pTM61 was prepared by methods as previously described[2].

***B. burgdorferi* transformations and screening.** The infectious *B. burgdorferi* strains used in these experiments were GCB726 (GFP)[2], and GCB776 (Tomato). All strains were grown for 48 h in BSK-II medium prepared in-house[5], in the presence of 1% mouse blood, except where noted[5]. For the generation of strains GCB726 and GCB776, electrocompetent infectious *B. burgdorferi* were prepared from strain B31 5A4 NP1 (ref. 6) as described[2]. The construction of strains GCB726 (infectious GFP) and GCB705 (non-infectious GFP) has already been reported[2]. Liquid plating transformations were performed with 50 µg pTM201 in the presence of 100 µg/ml gentamycin as described[7,8]. Gentamycin-resistant *B. burgdorferi* clones were screened for Tomato expression by conventional epifluorescence microscopy. PCR screening for native plasmid content was performed as described[9,10] and indicated that Tomato infectious *B. burgdorferi* strain used in this study contained all endogenous plasmids except cp9, which was displaced by the cp9-based pTM201 constructs. Non-transformed infectious *B. burgdorferi* (B31 5A4 NP1) induced identical immune responses to transformed *B. burgdorferi*.

Preparation of fluorescent *B. burgdorferi* for injection. As previously described[2], for each experiment infectious fluorescent *B. burgdorferi* strains were freshly inoculated from glycerol stocks into 15 ml BSK-II medium containing 6% rabbit serum and 100 µg/ml gentamycin. *B. burgdorferi* were grown to 5×10^7/ml, then diluted to 1-2 $\times$ 10^6/ml in BSK-II medium containing 6% rabbit serum, 100 µg/ml gentamycin, 1× *Borrelia*

antibiotic mixture (20 µg/ml phosphomycin, 50 µg/ml rifampicin and 2.5 µg/ml amphotericin B, prepared from individual antibiotics obtained from Sigma) and 1% Balb/c mouse blood. Spirochetes were grown in the mouse blood for 48 h at 35°C to a final density of ~5×10^7/ml. *B. burgdorferi* were pelleted (6,000 × g for 15 min at 4°C), washed twice in PBS (Invitrogen Canada), and resuspended to 2×10^9 *B. burgdorferi*/ml in PBS. In preliminary experiments, non-infectious GFP-expressing *B. burgdorferi* (strain GCB705) and *B. burgdorferi* grown in the absence of blood were examined for immune responses. Although the spirochetes and *i*NKT cells had strikingly different morphology, to avoid the possible confusion between GFP-expressing *B. burgdorferi* and GFP-expressing *i*NKT cells in some cases the bacteria were Syto 60-labeled and a Cy5 laser/635 nm filter was used. In addition, success with Tomato expression in *B. burgdorferi* allowed us to confirm our observations with a second label.

Quantitative analysis of phagocytic capacity. To examine which cell types capture foreign molecules *in vivo*, polychromatic microspheres (0.5×10^8; Polysciences), Syto 60-labeled *E. coli* (1.6×10^8; kindly provided by E.A-V., University of Guelph), and Syto 60-labeled *B. burgdorferi* (0.5×10^8) were administered intravenously. At 1 or 2 h after the injection, the binding capacity of hepatic *i*NKT, Kupffer and endothelial cells were evaluated using intravital video imaging. At 2 h, 5 h, 8 h, 12 h, and 24 h after the spirochete injection, the number of GFP-expressing *B. burgdorferi* ingested by red labeled Kupffer cells in sinusoids per ×20 magnification field of view was counted. Similarly, ingestion of Tomato-expressing *B. burgdorferi* by *Cx3cr1*$^{gfp/+}$ Ito-dendritic cells was also counted.

Preparation and analysis of Kupffer cells, Ito cells and lymphocytes. Mouse Kupffer and Ito cells were prepared from livers of BALB/cj mice at 5 h or 8 h after *B. burgdorferi* injection. Kupffer and Ito cells were isolated by *in situ* collagenase/pronase perfusion and differential centrifugation on OptiPrep (60% (w/v) iodixanol; Axis-Shield PoC) density gradients[11,12]. Briefly, the abdominal cavity of anesthetized BALB/cj mice was opened to canulate the portal vein. The liver was perfused *in situ* first with Ca^{2+}-, Mg^{2+}-free HBSS, and then with HBSS containing 0.05% collagenase type IV (Worthington Biochemical Corp.), 0.025% pronase E (US Biological), and 0.02% DNase I (Roche Diagnostics) at a flow rate of 4 ml/min. After perfusion, tissue was further digested in HBSS containing 0.009% collagenase type IV, 0.009% pronase E, and 0.02% DNase I at 37℃ for 30 min. The cell suspension was passed through a 90-micron nylon filter and centrifuged at 25 × g for 5 min at room temperature to remove the hepatocytes. The supernatant was transferred to a new tube and centrifuged at 400 × g for 10 min at 4℃. Subsequently, the cell pellets were resuspended in 15% iodixanol solution[11], and centrifuged at 400 × g for 15 min at 20℃. From this non-parenchymal fraction Kupffer cells were positively selected with anti-F4/80 microbeads and MACS column. Ito cells were purified through 17% (w/v) iodixanol gradient centrifugation[12] and MACS-based negative selection using anti-F4/80 microbeads. Cell purities of isolated Kupffer cells and Ito cells were around up to 95% and 85%, respectively as assessed by flow cytometry using anti-F4/80 and anti-GFAP (N-18; Santa Cruz Biotechnology), respectively.

Liver- and spleen-derived lymphocytes were isolated from *Cxcr6*$^{gfp/+}$ mice using a method previously described[13]. Briefly, livers and spleens were excised and finely

minced in a digestive medium containing 0.05% collagenase type IV (Worthington Biomedical Corp.) and 0.002% DNase I in HBSS. After gentle agitation at 37℃ for 30 min, the concentrate was passed through a 30-micron nylon filter and washed twice with ice-cold PBS (pH 7.4) and centrifuged at 300×*g* for 10 min. Lymphocytes were purified by a 37%/70% Percoll gradient and were negatively selected with anti-Gr-1 (RB6-8C5; eBioscience), anti-F4/80, anti-CD19 (1D3; eBioscience), and anti-CD8a (53-6.7; eBioscience) microbeads and MACS column to remove neutrophils, macrophages, B cells, and $CD8a^+$ cells, respectively. For experiment with a pure *i*NKT cell population, isolated lymphocytes from livers and spleens of 6-8 $Cxcr6^{gfp/+}$ mice were negatively selected using MACS column as described above, and TCRβ- and GFP^+ cells were sorted. Purity of isolated *i*NKT cells was >95%.

Lymphocytes (or pure *i*NKT cells) were grown in DMEM containing 10% FCS for 12 h, and 2×10^5 lymphocytes (or 5×10^4 *i*NKT cells) were seeded in 96-well round bottom plates. For CD69 and IFN-γ assay, Kupffer cells or Ito cells isolated at 8 h after *B. burgdorferi* infection were added at a concentration of 1×10^5 (for lymphocytes) or 5×10^4 (for pure *i*NKT cells) per well in a final volume of 200 μl complete DMEM medium and plates were incubated at 37℃ and 5% CO_2. At 6 h, 12 h, 24 h and 4 d after coculture, cells were collected for the analysis of CD69 expression, and the concentration of IFN-γ in the supernatants was determined by enzyme-linked immunosorbant assay (ELISA) kit (BD PharMingen) at 4 d after co-culture.

For CXCL9 assay, 1×10^5 Kupffer cells (per well) infected by *B. burgdorferi* were incubated at 37℃ and 5% CO_2, the supernatant were analyzed using ELISA kit (SABiosciences).

Flow cytometry. Lymphocytes or *i*NKT cells were collected from culture plates and resuspended in flow cytometry buffer (1% FCS, 0.05% sodium azide in PBS). Cells were incubated with phycoerythrin-conjugated anti-CD69 (H1.2F3; eBioscence) at 4℃ for 30 min, and washed in the buffer for flow cytometry and analyzed with a FACSCalibur (BD Bioscience) and CellQuest software. For CD1d expression of Kupffer cells and Ito cells FITC- or phycoerythrin-conjugated anti-CD1d was used.

Measurement of *B. burgdorferi* DNA in the tissue. Three days after infection with *B. burgdorferi*, mice were sacrificed, and organs and tissues were harvested, weighed, snap-frozen in liquid nitrogen, and stored at -80℃. DNA was collected from pre-weighed tissue samples using the Qiagen DNeasy kit (Qiagen Inc.), according to the manufacturer's instructions for isolation of DNA from blood and tissues. DNA was collected from 100 µl of blood or between 3-10 mg of tissue, to prevent saturation of DNA purification columns. For each tissue, aliquots of DNA from each mouse in a single experimental group were pooled together and mixed well by vortexing prior to Q-PCR, to reduce the total number of samples analyzed and permit analysis of an entire set of experimental samples in a single 96-well run using one set of quantification standards. Pooled samples and DNA standards were analyzed in duplicate by Q-PCR. DNA standards were prepared by amplifying target *B. burgdorferi* DNA sequence (from the *flaB* gene), using Q-PCR primers (see below), and cloning the resulting PCR product into the pJET1.2/blunt cloning vector using the CloneJet PCR cloning kit (Fermentas). The resulting DNA standard clone was verified by sequencing, and serial dilution was used to

prepare a set of standards ranging from 1-10^8 gene copies per 2 µl DNA sample. In this copy number range, amplification of DNA by Q-PCR was linear and quantitative.

Q-PCR was performed on 2.5 µl pooled sample DNA in 25 µl reaction volumes in a Bio-Rad IQ5 multicolor real-time PCR detection system, using methods and primers adapted from previous studies in which Q-PCR was used to quantify the relative number of *Borrelia* in different host tissues[14,15]. The primers used to amplify *B. burgdorferi flaB* DNA were: B1672 (5'-gcagctaatgttgcaaatcttttc-3') and B1673 (5'-gcaggtgctggctgttga-3'). Each primer was used at a final concentration of 400 nM. Reactions were performed in 1X iQ SYBR Green Supermix (Bio-Rad Laboratories, Mississauga, Ontario), prepared according to manufacturer's instructions. Temperature gradient PCR followed by melt-curve analysis was used to determine the optimal annealing temperature (60℃). PCR conditions: Step 1: 95℃ 3 min; Step 2: 45 cycles of 95℃ 15 sec, 60℃ 30 sec, 72℃ 20 sec; Step 3: melt curve analysis over melting range 53℃ to 95℃. All analysis of *flaB* gene copy number in experimental DNA samples was carried out in duplicate on plates with a duplicate set of standards ranging from 1-10^8 gene copies/well. The number of copies of *flaB* present in each experimental sample was normalized to the weight of the tissue sample from which total DNA was extracted. Q-PCR was also used to analyze the number of mouse *nidogen* gene copies per sample, but *flaB* copy numbers were not normalized to *nidogen* copy numbers because of differences in total amounts of DNA present in different tissues.

REFERENCES

1. Norman, M.U., Hulliger, S., Colarusso, P., Kubes, P. Multichannel fluorescence spinning disk microscopy reveals early endogenous CD4 T cell recruitment in contact sensitivity via complement. *J. Immunol.* **180**,510-521 (2008).

2. Moriarty, T.J. *et al*. Real-time high resolution 3D imaging of the Lyme disease spirochete adhering to and escaping from the vasculature of a living host. *PLoS Pathog.* **4**, e1000090 (2008).

3. Shaner, N.C. *et al*. Improved monomeric red, orange and yellow fluorescent proteins derived from *Discosoma* sp. red fluorescent protein. *Nat. Biotechnol.* **22**, 1567-1572 (2004).

4. Eggers, C.H. *et al*. Identification of loci critical for replication and compatibility of a *Borrelia burgdorferi* cp32-based shuttle vector for the expression of fluorescent reporters in the Lyme disease spirochete. *Mol. Microbiol.* **43**, 281-295 (2002).

5. Barbour, A.G. Isolation and cultivation of Lyme disease spirochetes. *Yale J. Biol. Med.* **57**, 521-525 (1984).

6. Kawabata, H., Norris, S.J., Watanabe, H. BBE02 disruption mutants of *Borrelia burgdorferi* B31 have a highly transformable, infectious phenotype. *Infect. Immun.* **72**, 7147-7154 (2004).

7. Bankhead, T., Chaconas, G. The role of VlsE antigenic variation in the Lyme disease spirochete: persistence through a mechanism that differs from other pathogens. *Mol. Microbiol.* **65**, 1547-1558 (2007).

8. Yang, X.F., Pal, U., Alani, S.M., Fikrig, E., Norgard, M.V. Essential role for OspA/B in the life cycle of the Lyme disease spirochete. *J. Exp. Med.* **199**, 641-648 (2004).

9. Tourand, Y. *et al*. Differential telomere processing by *Borrelia* telomere resolvases *in vitro* but not *in vivo*. *J. Bacteriol.* **188**, 7378-7386 (2006).

10. Purser, J.E., Norris, S.J. Correlation between plasmid content and infectivity in *Borrelia burgdorferi*. *Proc. Natl. Acad. Sci. USA* **97**, 13865-13870 (2000).

11. Brouwer, A., Hendricks, H.F.J., Ford, T., Knook, D. L. Centrifugation separations of mammalian cells In Preparative centrifugation – a practical approach (ed. Rickwood, D.) IRL Press at Oxford University Press, Oxford, UK, pp 271-314 (1991).

12. Shek, F.W-T. *et al*. Expression of transforming growth factor-β1 by pancreatic stellate cells and its implications for matrix secretion and turnover in chronic pancreatitis. *Am J Pathol* **160**, 1787-1798 (2002).

13. Ajuebor, M.N., Hogaboam, C.M., Le, T., Swain, M.G. C-C chemokine ligand 2/monocyte chemoattractant protein-1 directly inhibits NKT cell IL-4 production and is hepatoprotective in T cell-mediated hepatitis in the mouse. *J. Immunol.* **170**, 5252-5259 (2003).

14. Tupin, E. et al. NKT cells prevent chronic joint inflammation after infection with *Borrelia burgdorferi*. *Proc. Natl. Acad. Sci. USA* **105**, 19863-19868 (2008).

15. Benhnia, M.R. *et al*. Signaling through CD14 attenuates the inflammatory response to *Borrelia burgdorferi*, the agent of Lyme disease. *J. Immunol.* **174**, 1539-1548 (2005).